Sensors and Actuators B 266 (2018) 674–684

Contents lists available at ScienceDirect

Sensors and Actuators B: Chemical

journal homepage: www.elsevier.com/locate/snb

The impacts of water vapour and co-pollutants on the performance of electrochemical gas sensors used for air quality monitoring

Xiaobing Pang[a,*], Marvin D. Shaw[b,c], Stefan Gillot[b], Alastair C. Lewis[c]

[a] Key Laboratory for Aerosol-Cloud-Precipitation of China Meteorological Administration, College of Atmospheric Physics, Nanjing University of Information Science & Technology, Nanjing, 210044, China
[b] Wolfson Atmospheric Chemistry Laboratories, Department of Chemistry, University of York, York, YO10 5DD, UK
[c] National Centre for Atmospheric Science, University of York, York, YO10 5DD, UK

ARTICLE INFO

Article history:
Received 1 August 2017
Received in revised form 13 March 2018
Accepted 23 March 2018
Available online 29 March 2018

Keywords:
Electrochemical gas sensors
Low cost sensors
Air quality
Ozone
Nitrogen dioxide
Carbon monoxide

ABSTRACT

The analytical performance of low cost air pollution sensors under real-world conditions is a key factor that will influence their future uses and adoption. In this study five different electrochemical gas sensors (O_3, SO_2, CO, NO, NO_2) are tested for their performance when challenged with cross interferences of water vapour and other gaseous co-pollutants. These experiments were conducted under both controlled laboratory conditions and during ambient air monitoring in urban background air at a site in York, UK. Signal outputs for O_3, SO_2 and CO showed a positive linear dependence on relative humidity (RH). The output for the NO sensor showed a negative correlation. The output for the NO_2 sensor showed no trend with RH. Potential co-pollutants (O_3, SO_2, CO, NO_2, NO and CO_2) were introduced under controlled conditions using gas standards and delivered to each sensor in series along with variable RH. A matrix of cross-interference sensitivities were established which could be used to correct sensor signals. Interference-corrected sensor responses were compared against reference observations over an 18-day period. Once cross interferences had been removed the corrected 5 min averaging data for O_3, CO, NO and NO_2 sensors showed good agreement with the reference techniques with r^2 values of 0.89, 0.76, 0.72, and 0.69, respectively. The SO_2 sensor could not be evaluated in ambient air since ambient SO_2 was below the sensor limit of detection.

1. Introduction

Poor air quality is linked to over seven million premature deaths each year [1] and 96% of urban citizens are exposed to higher levels of air pollution than is recommended [2]. The public are increasingly aware of the health effects of air pollution but even in the most developed cities spatially resolved urban air quality measurements are currently limited. Low cost gas sensors have been presented as a technology that may bridge spatial gaps in air quality observations. Gas sensors take observations into new challenging environments and offer a potential means to monitor air pollution exposure on a person. [3,4]. Some recent air pollution sensor applications include the use of commercial semiconducting oxide ozone sensors for surface O_3 monitoring in a high spatial density in a valley of New Zealand [5]. The sensor data in that case were simply judged to be valid if the data passed three scientific criteria, where no further treatments were conducted to correct those data. As a result the differences between sensors and reference analysers had a standard deviation of 6 ppb in the field over several months [5]. Portable gas sensors were used to capture the spatial variability of traffic-related air pollutants through measurements at 76 sensor sites in a Canadian city [6]. It was found that sensors tended to overestimate the NO_2 and O_3 concentrations and the sensor data were corrected based on the correction equations between sensor and a reference analyser in fixed-station [6]. A custom, compact, laser-based methane sensor was coupled to an unmanned aerial vehicle to quantify fugitive methane emissions above a compressor station of natural gas [7]. Side-by-side intercomparison of the laser-based CH_4 sensor on aircraft and a ground-based reference analyser showed a good agreement between the instruments, which implied that the optical gas sensors would be less interfered by ambient environment factors. A black carbon sensor combined with a smartphone with GPS has been employed to estimate personal exposures to residential air pollution and public transportation emissions [8]. The above-mentioned examples show potential applications and pollutants, but data biases arising from sensors has not been fully

* Corresponding author.
E-mail address: pangxbyuanj@163.com (X. Pang).

https://doi.org/10.1016/j.snb.2018.03.144

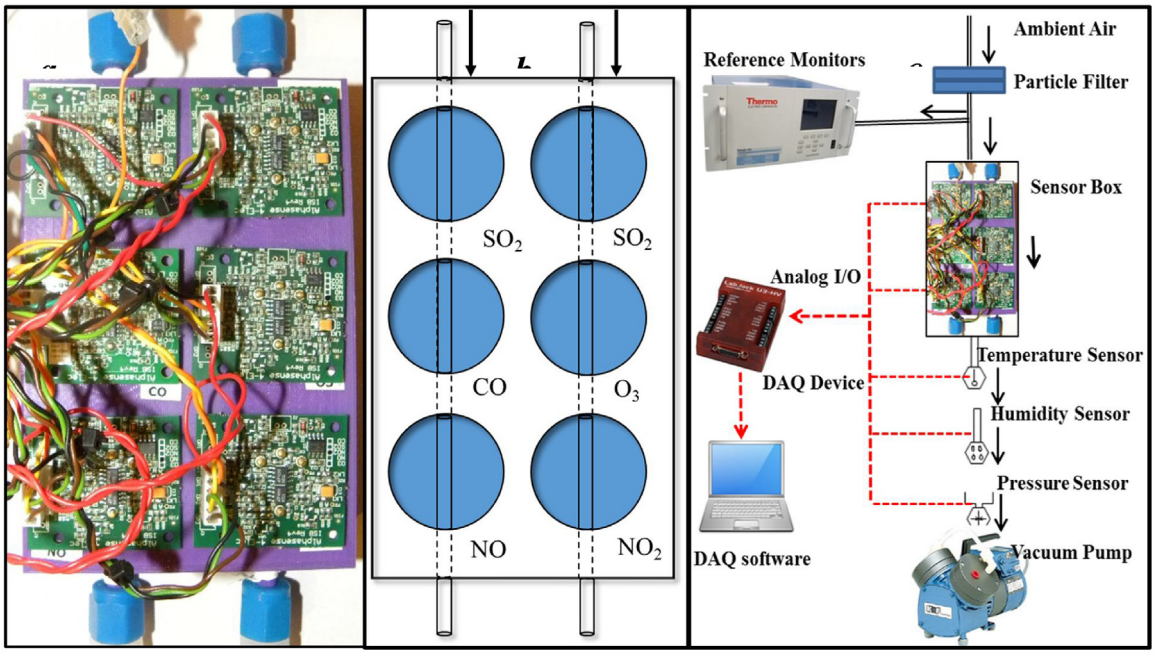

Fig. 1. Schematic diagram of sensor box and the experimental setup for the performance tests of the sensor box. Panel ***a***: the photograph of sensor box, panel ***b***: the schematic diagram of sensor box with sensor locations and its sampling gas flows, panel ***c***: the experimental setup of sensor box and reference instruments in air quality monitoring.

described, and this is considered a source of uncertainty that act currently as a barrier to more widespread adoption.

A key requirement in the future development of low cost sensors and related applications is an appropriate knowledge base on their performance and their fit to particular purposes [9]. The rapid rate of technological evolution by some manufacturers makes this challenging for the academic community to keep pace with, since regular updates to sensor technologies occur. Of the various classes of gaseous air pollution sensor being used in higher specification/higher quality commercial devices, electrochemical sensors are probably the most common. The potential limitation of electrochemical gas sensors when used in ambient air monitoring is their chemical selectivity to the measurand, and this is sometimes lower than the existing recognised reference measurement techniques [10,11]. Previous studies have showed for example a cross-interference from ambient O_3 to certain electrochemical NO_2 sensors (NO_2-B42, Alphasense, UK) and the baseline responses of the sensors have been seen to be influenced by meteorological conditions including air temperature and humidity [12–14]. The degree of interference from variable atmospheric CO_2 when presented as a co-pollutant to a group of O_3, SO_2, NO, and NO_2 sensors was reported in [11]. Calibration responses of gas sensors tested in the lab and in the field have been reported to be often different, with relationships observed in the field that are only applicable to a particular location/chemical climatology and also for a limited period of time [15].

Methodologies that can correct for interferences to sensor responses in complex real ambient air are available including machine learning methods, and through more traditional analytical regressions of sensor response [9,11,12,16]. Inaccuracies in gas sensor detection of air pollution can potentially arise are due to the diffusion into the sensor cell of other chemicals which may either generate additional electrical signals or suppress response. To obtain a more true sensor measure of the target gas requires an estimation of the cumulative interference signals (both positive and negative) and their removal from the raw sensor signal [17,18].

In this study the effects of relative humidity and several other trace atmospheric components including O_3, SO_2, CO, CO_2, NO and NO_2 on five commonly used electrochemical gas sensors (O_3, SO_2, CO, NO, and NO_2) were determined as cross-sensitivities in the laboratory. Those sensors were further deployed in an 18-day field trial alongside with some reference air pollution apparatus. Using the cross–sensitivity values we managed to correct sensor signals to eliminate the potential interferences from co-pollutants with the help of reference instruments.

2. Experimental

2.1. Gas sensors

Five commercially available electrochemical gas sensors were all purchased from Alphasense Ltd (Essex, UK) CO (CO-B4), O_3 (OX-B431), NO (NO-B4), NO_2 (NO_2-B42) and SO_2 (SO_2-B4). These sensors are based on electrochemical reactions that take place within the sensor between gases and a certain electrolyte. The electrochemical sensor has working electrode (WE), auxiliary electrode (AE) and counter electrode (CE). The AE is used to correct for zero potential changes. The resulting voltage between WE and CE is the signal potential from the target gas measurement. An individual sensor board (ISB) is preconfigured for each individual sensor with fixed zero and electronic gain (sensitivity in voltage/ppb). The circuit board provides buffered voltage outputs from both WE and AE with lowest noise. All sensors were housed into a homemade flow cell device (Fig. 1a and b), through which the calibration gas or ambient air were introduced to the sensor heads simultaneously under controlled conditions. All gas lines were ¼" (inch) PTFE (Polytetrafluoroethylene) tubing with stainless steel fittings (Swagelok, USA). A LM35 temperature sensor (Texas Instruments), a HIH-4000-001 humidity probe (Honeywell) and a MPX4200A absolute pressure sensor (Freescale Ltd) was employed to measure the inline temperature, relative humidity, and atmospheric pressure, respectively (Fig. 1c). The sensor box was kept inside the laboratory, in which air temperature was controlled and stable at $20 \pm 1\,^{\circ}C$ during the periods of both the laboratory study and the ambient air monitoring exercise.

2.2. Data acquisition

All sensor boards were connected through a LabJack data-acquisition (DAQ) device (U6 Series, LabJack Corporation, USA) to our in-house designed LabVIEW DAQ software (LabVIEW 2012, National Instrument, USA) (Fig. 1c). Through this software the WE and AE potentials of each sensor were monitored and converted into gas mixing ratios (ppb). The detailed description can be seen in our previous paper [13].

2.3. Interferences from humidity and cross interferences in air

In this study the influence of humidity on the gas sensors was initially investigated through testing the variations of sensor WE and AE potentials in clean 'zero air' at different controlled relative humidity (RH, 15%, 30%, 45%, 60%, 75% and 80%). A pure air generator (PAG003, Eco-physics) was used to create the initially dry zero air in this experiment. The zero air from the generator contained less than 10 ppt NO, NO_2, O_3, SO_2 and CO. The humidity of zero air was then adjusted to target values using a dew point generator (DG-3, Michell Instruments, UK). The period of testing for each RH set-point varied from 5 min to 10 min as shown in Fig. 2 and after each test period the RH changed in a step-wise manner. The sensor signals in zero air were seen to change significantly with RH variations and these effects were then quantified as a sensor cross-sensitivities with the unit of volts/% RH).

The sensors were then calibrated to their target gases, and simultaneously to the other five co-pollutants, at five different RHs (15%, 45%, 60%, 75% and 85%). The slopes of those sensor responses were then used to determine the sensitivities to target gases and the cross-sensitivities to the co-pollutants. The mole fractions chosen for sensor calibrations were:

0, 25, and 50 ppb for CO,
0, 50, 100, 150 ppb for O_3,
0, 20, 40, 80, and 160 ppb for NO,
0, 80, 140, 280, and 360 ppb for NO_2,
50, 75, 100, 125 ppm for CO_2 and,
0, 50, 100, 150, and 200 ppb for SO_2.

The different blends of NO, NO_2, SO_2, CO, and CO_2 in zero air were generated by directly diluting binary standard mixtures at high mixing ratios (5 ppm NO, 5 ppm NO_2, 10 ppm SO_2, 500 ppb CO and 10 ppm CO_2) from BOC (Guildford, UK), with zero air using a gas dilution device (Multi-gas calibrator, S6100, Monitor Europe). A multi-gas calibrator with an internal O_3 generator was used to produce O_3 gas in air in different mixing ratios for the sensor calibrations.

2.4. Sensors and reference instruments in air quality monitoring

For a comparison of sensors in external air, samples were drawn from a building height manifold into reference instruments housed in the same lab as the sensors. A UV photometric O_3 analyser (Model 49C, Thermo Electron Corporation, USA) was used for the reference measurement for O_3. The calibration of the instrument was carried out using an Ozone Primary Standard (Model 49i-PS, Thermo Fisher Scientific Inc., USA), which itself is certified yearly by the UK National Physical Laboratory (NPL). Reference measurements for NO_X were made using a high sensitivity NO_X instrument (Air Quality Design Inc). A more detailed description of the NO_X instrument can be found in a previous study [19]. A SO_2-H_2S analyser (Model 450i, Thermo Electron Corporation, USA) was used as the reference measurement for SO_2. The reference apparatus for CO_2 was an SRI 8610C gas chromatograph (Torrance, USA) with a flame ionisation detector (FID) with a time resolution of 5 min. The reference measurements for H_2 and CO were by TA3000R RGD gas analyser (AMETEK Process Instruments, Swindon, UK). The above-mentioned reference analysers were the same instruments as those deployed in the standard gas measurements during the laboratory experiments of sensor sensitivities and cross-sensitivities.

To evaluate the real-world applicability of the lab-derived correction factors and sensor performance, the sensors were deployed for ambient air quality monitoring alongside the reference instruments during an 18-day monitoring exercise (from 7th to 25th August 2015). The sampling site was the campus of University of York, UK and the air sample was drawn from 10 m above ground level using a stainless-steel diaphragm metal bellow pump (Senior Aerospace, MB302) at a flow rate of 1.0 L/min to the gas hood of each sensor through a ¼" PTFE tubing. Sensor data and reference measurement data were averaged to 5-min intervals and evaluated over the 18-day period.

Average mixing ratios of atmospheric compositions in ambient air measured during the whole campaign period by the reference methods were 23 ± 12 (average $\pm$ SD) ppb for O_3, 1.3 ± 7.2 ppb for NO, 5 ± 0.2 ppb for NO_2, 0.2 ± 0.1 ppb for SO_2, 106 ± 24 ppb for CO, 676 ± 161 ppb for H_2 and 389 ± 24 ppm for CO_2, respectively. The minute-averaged temperature and the relative humidity in the sampled air were $20.2 \pm 0.7\,^{\circ}C$ (average $\pm$ SD) and $59 \pm 12.1\%$ (average $\pm$ SD) during the field campaign (Fig. 3).

3. Results and discussion

3.1. Interferences to electrochemical sensors

Although ambient temperature is known to be a major factor that can affect sensor response performance, in this study the effects of temperature are not explored further, and all experiments are conducted under a single set of controlled conditions. The inline gas temperatures and sensor body temperatures were both stable at $20 \pm 1\,^{\circ}C$. As Fig. 3 shows the variation of RH is considerable during two weeks from less than 40% to more than 80% though inline gas temperature kept at a fixed value.

3.1.1. Relative humidity effects

Fig. 2a,c,e,g, and i show the electrode voltages of WE and AE of each sensor when exposed to zero air in the presence of varying RH. These experiments are used to first demonstrate that the 'zero' value used for this set of sensors is not constant, but needs adjustment to reflect ambient RH. This is significant since several approaches for field calibration of sensors have proposed bootstrapping ambient sensor measurements to either nearby reference instruments or the sensor ensemble, but such an approach must assume a constant zero value to deliver a calibration slope. The resulting signal voltages (WE-AE) of sensors show a range of relationship with the RH in sample air, (Fig. 2b,d,f,h, and j as well as their calibration equations). The slopes of those zero air baselines to RH are reported in the unit of V (RH%) $^{-1}$ or mV (RH%)$^{-1}$.

As an example, Fig. 2a shows the sensor voltages of WE and AE for the O_3 sensor increasing with RH. The increases in WE are significantly greater than those of AE, which results in the corrected sensor zero signal outputs (WE-AE) displaying a positive correlation with RH with R^2 of 0.85 (Fig. 2b) and a slope of 0.56 mV (RH%) $^{-1}$. We note that over very short timescales voltages of WE can rapidly jump (in the example to 0.26 V from 0.18 V) and then slowly decrease to a stable value of 0.22 V over a period of 60 s during the initial period of RH change to 30% from 15% (Fig. 2a). In the ambient atmosphere, such rapid changes in RH would not often occur, but this rate of change could well be experienced if a sensor was carried on a person from outdoors to in, or vice versa.

For the CO sensor, the voltage of WE slightly increased to 0.47 V at RH of 85% from 0.42 V at RH of 15% whilst AE had a negative relationship with the RH increment decreasing to 0.31 V at 85% RH from

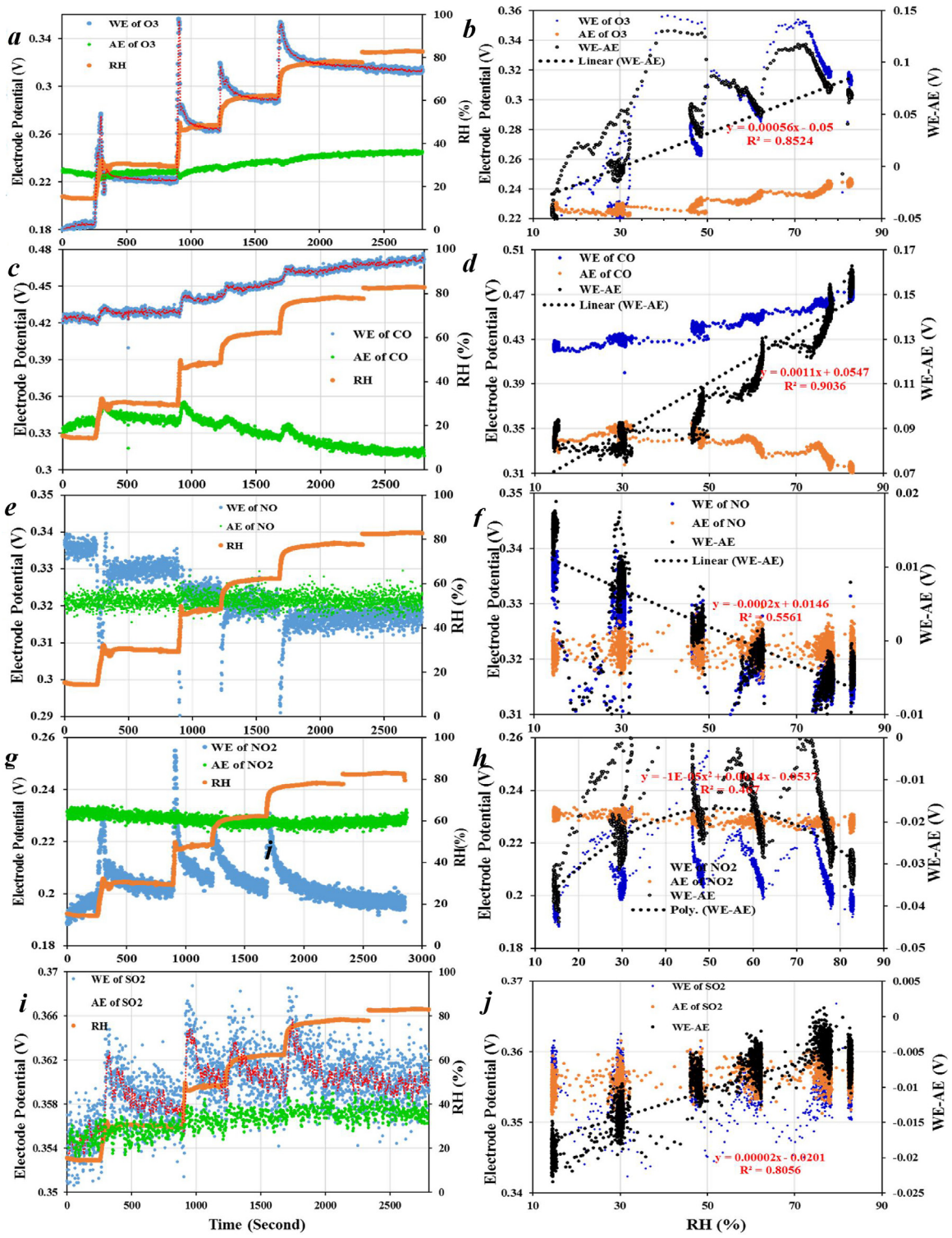

Fig. 2. RH effects on the sensor work electrode (WE) and analogue electrode (AE) signals (voltage) for OX-B431O_3 (panel ***a***), CO-B4 (panel ***c***), NO-B4(panel ***e***), NO_2-B4(panel ***g***), and SO_2-B4 (panel ***i***) sensors. The approximate relationship (black line) between sensor signal outputs (WE − RE) and RH for OX-B431O_3 (panel ***b***), CO-B4 (panel ***d***), NO-B4 (panel ***f***), NO_2-B4 (panel ***h***), and SO_2-B4 (panel ***i***) sensors, respectively.

0.34 V at 15% RH (Fig. 2c and d). The sensor signal output, voltage of (WE-AE), showed a positive correlation with RH increment with R^2 of 0.90 and a slope of 1.1 mV $(RH\%)^{-1}$.

For the NO sensor, the AE voltage varied little during the period of RH variation whilst the WE voltage gradually decreased with RH increments from 0.34 V at RH 15% to 0.32 V at RH 85% (Fig. 2e). The sensor voltage showed a negative correlation with RH increment with R^2 of 0.56 and a slope of – 0.3 mV $(RH\%)^{-1}$ (Fig. 2f). Similar to the ozone sensor WE voltages showed rapid short-term drops during the initial RH change and recovered to a stable level in around 30 s.

For the NO_2 sensor, the AE voltage remained constant during the RH variations. The WE signal output increased significantly in the first 1 min of each RH increment and gradually recovered to

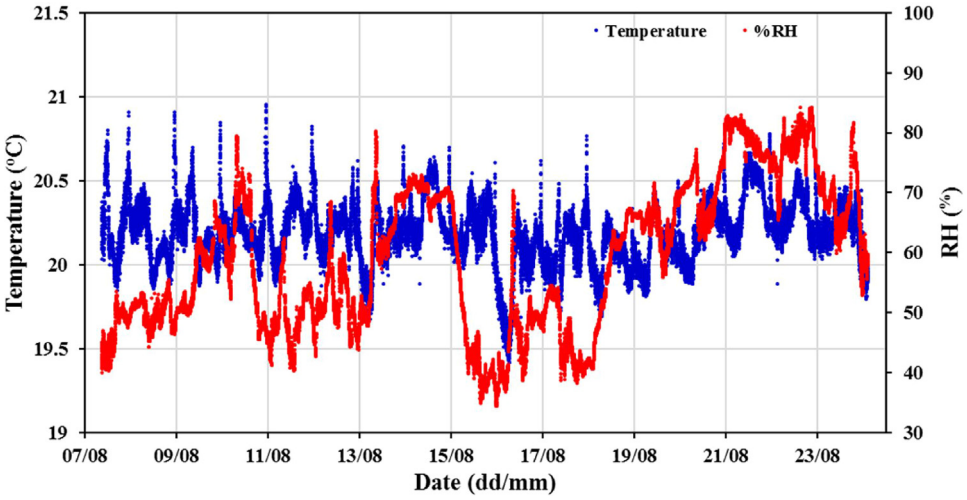

Fig. 3. Measured variations of temperatures and relative humidity (RH) in ambient air during the field campaign from 7 August 2015–25 August 2015. Temperature sensor was in a laboratory.

the stable value (Fig. 2g and h). The voltage of (WE-AE) at RH 15% was the same as the final value at RH 75% after 20 min recovery time indicating that at typical RH values this sensor zero value has relatively low sensitivity to RH.

For the SO_2 sensor, the AE voltage varied little during the period of RH change while the WE voltage gradually increased with the RH increments and jumped to a higher level at the beginning of each RH increment (Fig. 2i). The voltage of (WE-AE), showed a positive correlation with RH increment (Fig. 2j).

3.1.2. *Influences from co-pollutants under controlled conditions*

The response of an electrochemical gas sensor to gaseous species, other than the measurand, can be thought of as a cross-sensitivity. Since ambient air is a complex and variable matrix it is essential to quantify any cross-sensitivities and develop strategies to remove those signals before reporting a mixing ratio. In this study the cross-sensitivities of the sensors to five common co-pollutants are established using a fixed calibration gas composition containing the measurand, and then variable quantities of each co-pollutant, with each experiment then tested at four different RH values.

An 'ideal' selective sensor would show no change in response when presented with a constant mixing ratio of the measurand and a vary amount of either co-pollutant or RH, or both together. As is shown in Fig. 2, we already anticipate that there will be a different response for variable RH, so these experiments then test the additional effects of the co-pollutant.

This type of multi-dimensional experiment generates considerable data, and we only show plots and extended detail for one sensor, CO. The detailed calibration results for the CO sensor are shown in Fig. 4. In this experiment the sensor is exposed to a series of CO mole fractions in zero air, and then co-pollutants to CO sensor are varied over typical urban values. Fig. 4a is essentially the classical calibration plot from which CO sensor sensitivity per ppb can be derived from the slope. In Fig. 4b CO sensor responds to the increased mixing ratios of co-pollutant NO_2. The WE value from the CO sensor increases as the NO_2 increases – an artefact signal. There is no response of the CO sensor to increasing NO, slight upwards signals associated with CO_2 and O_3, and a negative response in the presence of increasing SO_2. Superimposed different lines are these cross-interference effects when the co-pollutant experiments are performed under different RH conditions. In general the behaviours of the CO when exposed to different pollutants are similar in at least sign, but the y-intercept values vary considerably due to different RH.

The detailed sensitivities and cross-sensitivities of all sensors and co-pollutants are summarised in Table 1 and the calibration curves were shown in the figures in supporting material. We would stress that the individual sensor sensitivities to their measurand gas at typical atmospheric mixing ratios is considerably higher than the sensor cross-sensitivities to other co-pollutants – typically by a factor of between 10–100 times. The exception is for the O_3 sensor which shows similar sensitivities to its target gas O_3 and the co-pollutant NO_2–a known phenomenon reported anecdotally by others[12].

The CO sensor shows small positive responses to O_3 and NO_2 and negative responses to CO_2 and SO_2 whilst demonstrating little cross-sensitivity to NO (Fig. 4). The SO_2 sensor displays some significant negative cross-sensitivity to O_3 and NO_2. The NO_2 sensor shows high selectivity since it has generally low cross-sensitivities to co-pollutants, although at the highest RH values and lower NO_2, elevated urban mixing ratios of CO_2 may induce an artefact signal. The NO sensor shows negative responses to O_3 and NO_2 at all RHs and a slight positive correlation to CO and SO_2. The O_3 sensor shows similar cross-sensitivities to O_3 and NO_2, which means NO_2 generates a large interference in the sensor. The O_3 sensor responds positively to the co-pollutants CO and CO_2 whilst negatively to SO_2 and NO. Compared with other three gas sensors, CO and NO_2 sensors show higher specificity to their target gases based on their lower values of cross-sensitivities. It should be noted the NO_2-B42F series electrochemical sensor is of a particular manufacturing generation and has since been replaced with the Alphasense NO_2-B43F series sensor which is less prone to this effect. The same type of caveat can be applied to all sensors – these experiments were conducted using the off-the-shelf devices available at the time, and later versions may well have different response characteristics.

3.2. *Correction for interferences*

Interferences effects from ambient co-pollutants and RH appears unavoidable with the current generation of electrochemical sensor devices, although may of course improve with future technologies. With knowledge of those effects, the next question is whether they can be removed through co-measurement and post-processing of data? According to the working principles of electrochemical gas sensors, the concentration (mixing ratio with unit of ppb) of target gas has a relationship with sensor signal and sensor sensitivity as shown in the equation of Eq. (1) [13]. Sensor signal is the voltage output from the sensor with unit of V, which

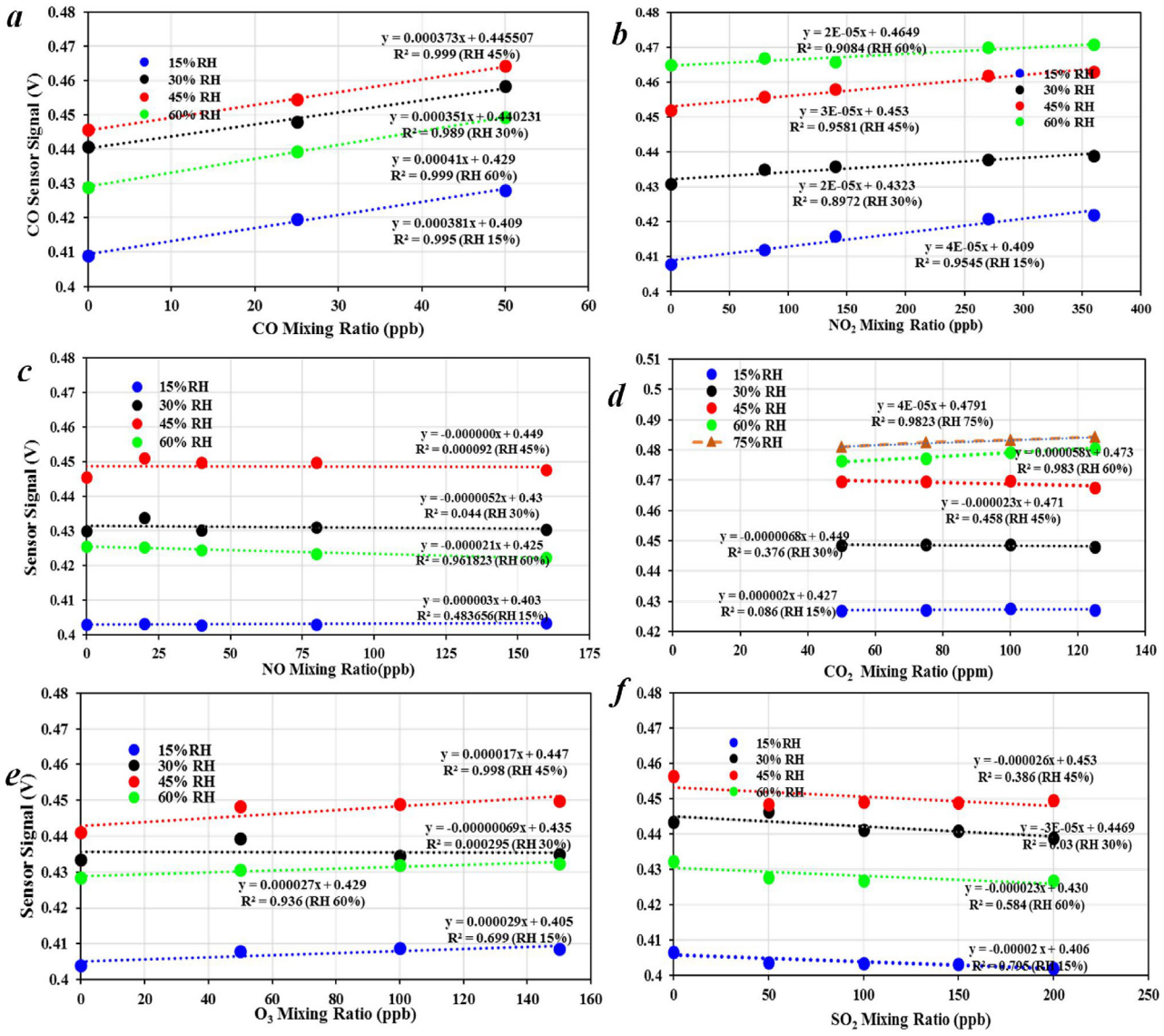

Fig. 4. CO-B4 sensor sensitivity to CO: slope of the calibration curve between sensor signal (voltage) and CO mixing ratio (panel ***a***) and its cross-sensitivities for different exposure to NO_2 (panel ***b***), NO (panel ***c***), CO_2 (panel ***d***), O_3 (panel ***e***) and SO_2 (panel ***f***) gases, and for different RHs of 15%, 30%, 45% and 60%.

is equal to the difference between voltage of working electrode (WE) and voltage of auxiliary electrode (AE). The sensor signal in Eq. (2) contains the interfering signals and should be corrected. The interfering signals from co-pollutants can be eliminated from the sensor signal as shown in Eq. (2), which are calculated by the products between sensor cross sensitivities with unit of V/ppb to co-pollutants and the co-pollutant mixing ratios with unit of ppb as illustrated in Eq. (3). The amount of co-pollutant species (n) in Eq. (3) is in theory equal to the number of co-existing gaseous species in the air where the gas sensor is deployed [11].

$$(\text{Gas Concentration}) = \frac{sensor\ signal}{Sensitivity} = \frac{(WE - AE)}{Sensitivity} \quad (1)$$

$$(\text{Gas Concentration})_{\text{corrected}} = \frac{(Signal)_{corrected}}{Sensitivity} = \frac{(Sensor\ Signal - Interfering\ signal)}{Sensitivity} \quad (2)$$

$$Interferingsignal = \sum_{i=0}^{n} MixingRatio_{copollutanti} * (CrossSensitivity)_i \quad (3)$$

We evaluated the scale of co-pollutant interferences and corrected the raw sensor data by removing the interference signals through a simple linear correction during the sensor deployments in an 18-day campaign of air quality monitoring. The assumption is that all interferences act in a step-wise manner and no non-linear additive or suppressive effects occur. The ambient RH (%) was measured by the humidity sensor while the mixing ratios (ppb) of SO_2, NO, NO_2, CO_2, CO and O_3, in the ambient air were provided by the high-quality reference instruments used in the lab calibrations.

The cross-sensitivities of each sensor to the co-pollutants are chosen from the values in Table 1 at the appropriate RH, which is close to the ambient RH. The corrected data after the subtraction of each co-pollutant effect from NO, NO_2, CO, CO_2, SO_2, and O_3 sensors are shown in Fig. 5. For the O_3 sensor the raw O_3 mixing ratios varying from 150 to 200 ppb (blue dots in Fig. 5a) are over 5–10 times higher than the final corrected data, which are mainly in the range

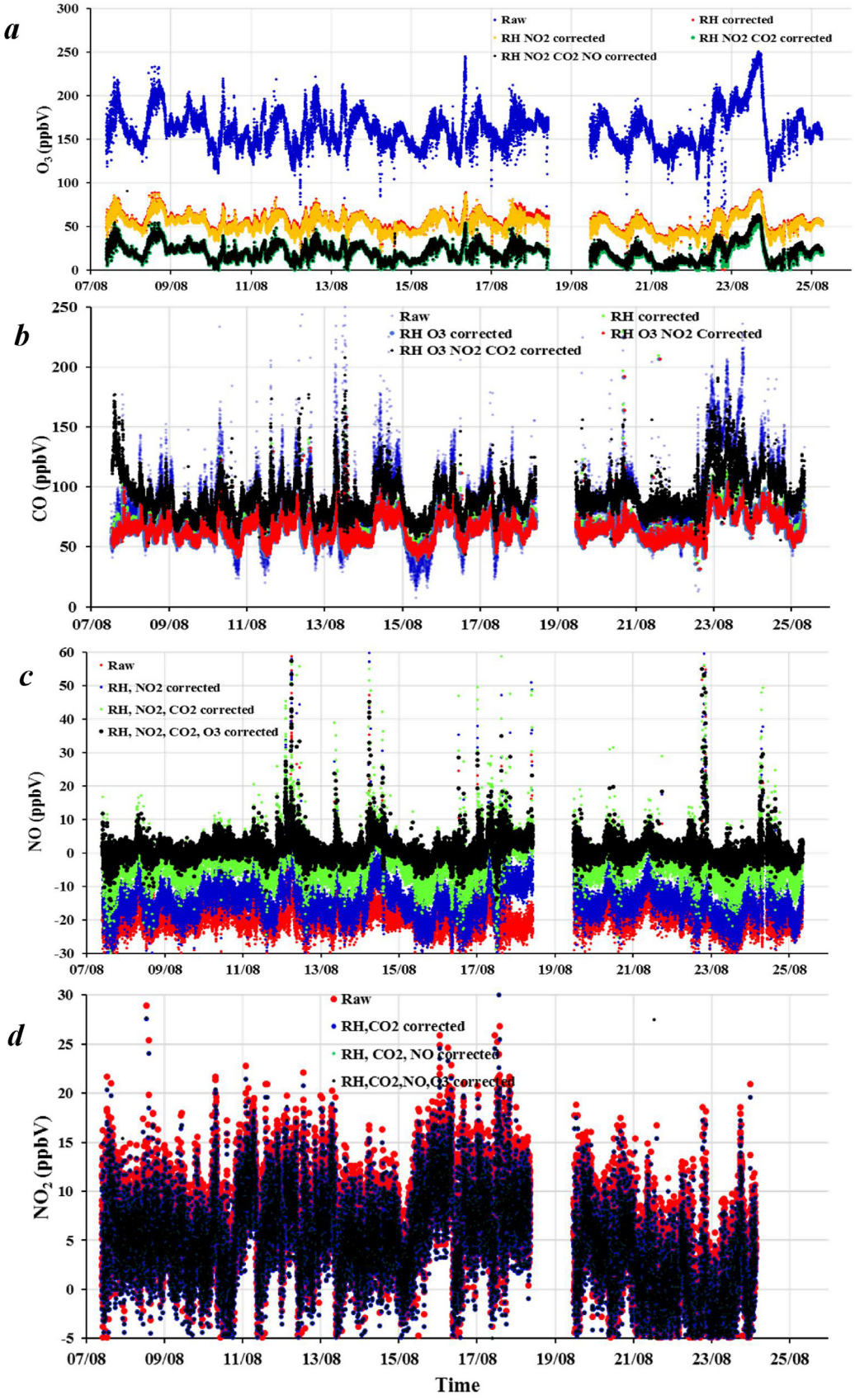

Fig. 5. Corrections of raw data (5-min averages) from OX-B431O_3 sensor (panel ***a***), CO-B4 sensor (panel ***b***), NO-B4 sensor (panel ***c***), and NO_2-B4 (panel ***d***), based on ambient air measurements during a field campaign (from 7 August 2015–25 August 2015).

Table 1
Sensor sensitivities to their target species (the data in grey shade in table, in units 10^{-3} V ppb^{-1}) and their cross-sensitivities to other copollutants (in 10^{-3} V ppb^{-1} for O_3, NO, NO_2, SO_2 and 10^{-3} V ppm^{-1} for CO_2) under four different RH conditions of 15%, 30%, 45% and 60%.

Target Gases	Sensor	OX-B421 O_3	CO-B4	NO-B4	NO_2-B4	SO_2-B4
	RH(%)					
O_3	15	0.44	0.029	-0.01	0.002	-0.14
	30	0.44	-0.0007	-0.01	0	-0.12
	45	0.43	0.017	-0.014	0	-0.14
	60	0.45	0.027	-0.009	-0.004	-0.15
CO	15	-0.025	0.37	-0.012	-0.035	0.010
	30	0.013	0.35	0.028	-0.012	0.015
	45	0.009	0.37	0.007	-0.007	0.013
	60	0.011	0.41	-0.004	0.005	0.054
NO	15	-0.21	0.003	0.54	-0.004	0.060
	30	-0.09	-0.005	0.57	-0.011	0.022
	45	-0.12	0	0.56	-0.013	0.027
	60	-0.11	-0.002	0.55	-0.009	0.019
NO_2	15	0.44	0.04	-0.09	0.42	-0.1
	30	0.43	0.02	-0.09	0.48	-0.1
	45	0.44	0.03	-0.1	0.43	-0.1
	60	0.44	0.02	-0.1	0.45	-0.1
SO_2	15	-0.022	-0.02	0.01	0.002	0.19
	30	-0.01	-0.03	0.006	0.005	0.21
	45	-0.015	-0.026	0.004	0.005	0.20
	60	-0.002	-0.023	0.007	-0.002	0.22
CO2	15	0.01	-0.002	-0.009	0.001	0.006
	30	0.04	-0.007	-0.0002	0.002	0.007
	45	0.1	-0.023	-0.014	0.004	0.012
	60	0.1	-0.058	-0.024	0.009	0.010
RH		0.56	0.11	-0.20	0.00	0.02

of 20–50 ppb (black dots in Fig. 5a). The humidity and CO_2 were the predominant interferences to O_3 sensor whilst the influence from ambient NO and NO_2 were insignificant (Fig. 5a). For the CO sensor RH and CO_2 were the predominant interferences (Fig. 5b). In previous study gaseous H_2 was found to be another important interference to the CO sensor [9].

For the NO sensor, the corrected data after each correction of co-pollutant interference increased gradually from the initial estimate of concentration since the cross-interferences from RH, CO_2, O_3 and NO_2 are negative values (Fig. 5c). The uncorrected data from the NO sensor varied in the range of −30 to −10 ppb whilst the final corrected data increased to the range of −5 to 10 ppb.

For the NO_2 sensor, only CO_2 interference was a major factor. The CO_2 interference for NO and O_3 was relatively insignificant. These can be seen in the corrected data shown in Fig. 5d.

3.3. Comparisons between corrected sensor data and reference data

The interference-corrected air quality monitoring sensor data is shown in Fig. 6 (black dots in panels) alongside with the reference data (red dots in panels). A linear regression was applied between the corrected sensor data, and the reference analyser data and the scatter plots of their correlation relationships are shown in Fig. 7 with the regression equations with intercepts and correlation coefficients (*R*-square). The R-square values imply that the corrected data from O_3, CO, NO and NO_2 sensors show good consistency with their reference measurements although the corrected values are a little lower than those from the reference instruments. The reason for the lower corrected sensor data may be the baseline of the sensors decreased gradually with the deployments, which was not corrected using this one-time correction method. The sensors may have to be corrected regularly with zero air to recover their baselines and standard gases and to check the sensitivities after a certain time deployment. The results in Figs. 6 and 7 indicate O_3, CO, NO and NO_2 sensor performances to be good and perfectly reasonable for general qualitative air quality monitoring after these corrections. The performance of SO_2 sensor is an exception and shown to be noisy compared with reference data (Fig. 6e). The SO_2 sensor could not be reasonably evaluated in the ambient air comparison since typical UK SO_2 mixing ratios in ambient air (< 1 ppb) were below to the sensor detection limit of 5 ppb.

4. Conclusions

A comprehensive evaluation of five electrochemical gas sensors often used in lower cost air quality monitors was performed using controlled exposure to co-pollutants in the lab and in a side-by-side ambient air test. The cross-interference from humidity and the co-pollutants in air on O_3, CO, NO, NO_2, and SO_2 sensors were quantitatively evaluated across a plausible range of mole fractions that might be found in polluted urban air. The interference sensitivity from co-pollutants was typically in the range 10 − 1% of the measurand under ambient conditions and showed a range of both signal enhancing and suppressing effects. For identical co-pollutant and measurand mixing ratios the effect of different RH was profound, often a much larger effect than the co-pollutant cross-sensitivity. Using simple linear regressions it was possible to recreate reference measurements reasonably well when the sensors were tested side-by-side over an 18-day summer field experiment. The interference signals from co-pollutants were calculated as the product of the cross-sensitivities and their mixing ratios and were removed

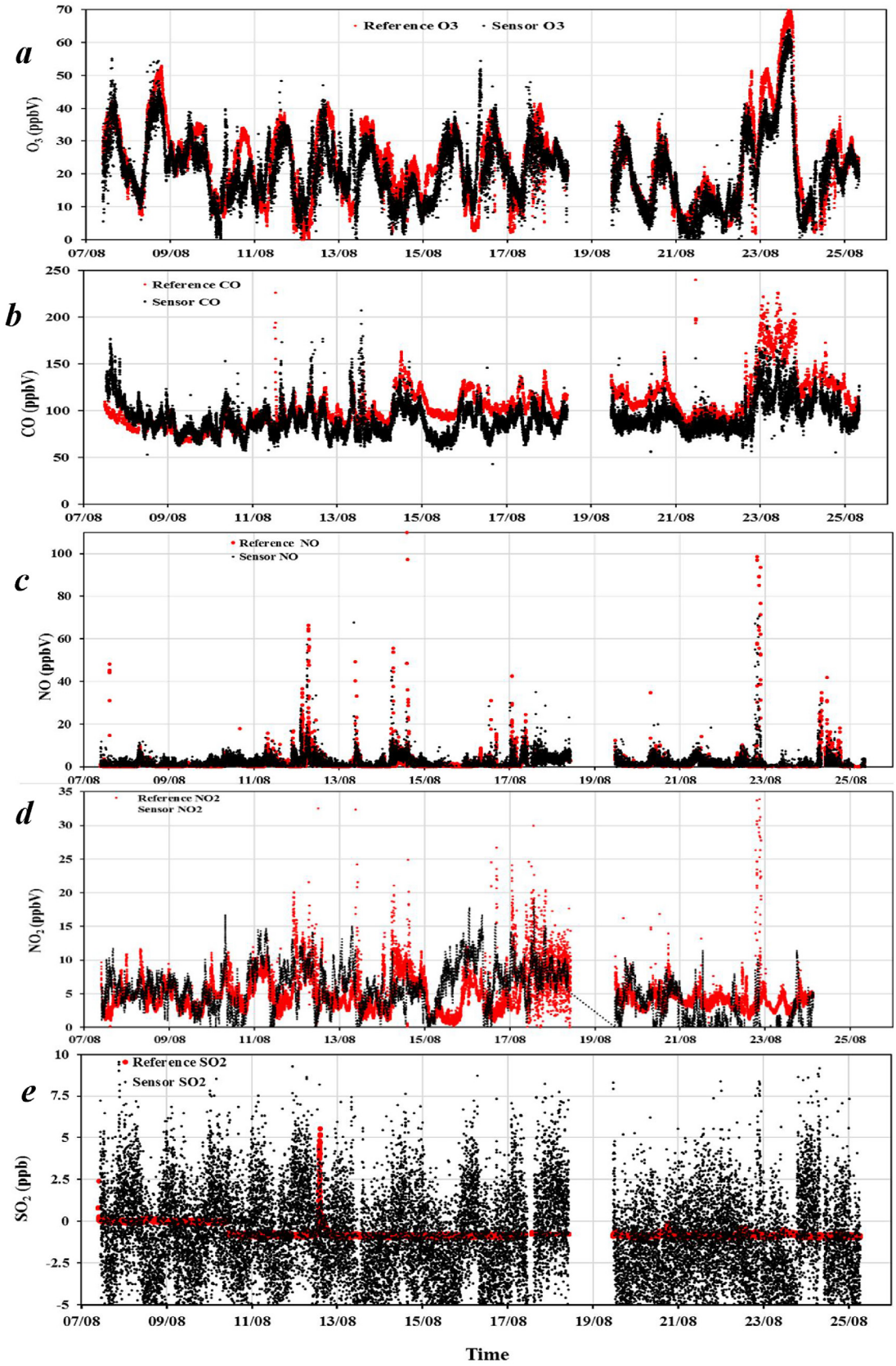

Fig. 6. Comparisons between the corrected sensor data (5-min average) (black dots) and the reference data (5-min average) (grey dots) during the 18-day field campaign. Panel ***a***: OX-B431O_3 sensor and a UV photometric O_3 analyser; panel b: CO-B4 sensor and a TA3000R RGD CO gas analyser; panel ***c***: NO-B4 sensor and a NO_X instrument; panel ***d***: NO_2-B4 sensor and a reference NO_X instrument; panel ***e***: SO_2-B4 sensor and a Thermo SO_2 Analyzer.

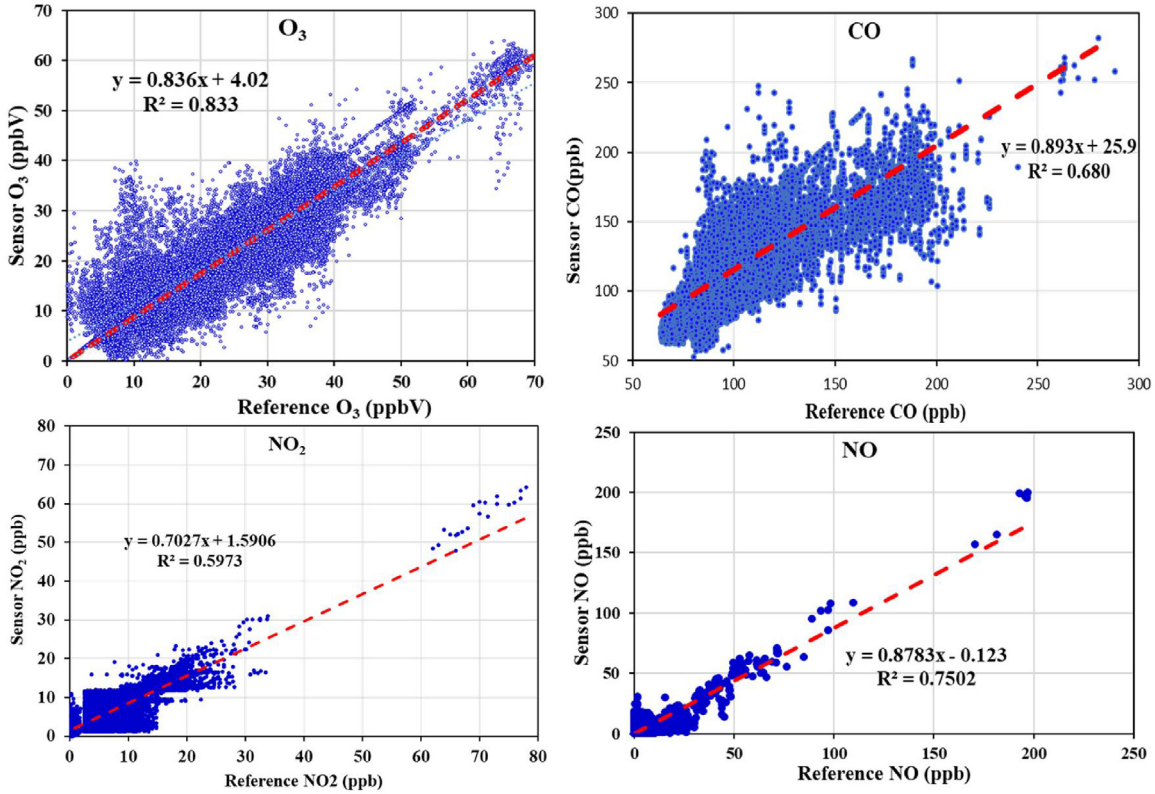

Fig. 7. The scatter plots of the correlation relationship between corrected sensor data and reference analyser data. The regression equations with intercepts and correlation coefficients are shown as well in the scatter plots.

from the sensor raw signals. The corrected sensor data for O_3, CO, NO and NO_2 sensors showed good overall agreements with the reference measurements, however ambient SO_2 mixing ratios were below the sensor detection limit and could not be evaluated. These results suggest that when used in isolation there remains considerable potential for sensor-reported air pollution mixing ratios to be affected by cross-sensitivities to other, often atmospherically correlated pollutants and to changes in RH. However, if reference measurements are available for comparison, for example where sensors are used to augment an existing urban network, then corrections can be made. It should be noted that the correction approach tested here uses a single factor for cross-interference that is applied over a short and fixed time scale (18 days). We have no evidence from these experiments that these correction factors would hold for longer periods of sensor deployment in the field, and this is an uncertainty that needs resolving in the future.

Acknowledgements

XP thanks the National Key Research and Development of China (2017YFC0209701) for financial support. This study is supported by the AIRPRO-Beijing NERC consortium project (NE/N007115/1) and NCAS/NERC ODA Foundation grant.

References

[1] W.H.O. (WHO), Air pollution estimates, (2014).
[2] S.S. Lim, T. Vos, A.D. Flaxman, G. Danaei, K. Shibuya, H. Adair-Rohani, et al., A comparative risk assessment of burden of disease and injury attributable to 67 risk factors and risk factor clusters in 21 regions, 1990–2010: a systematic analysis for the Global Burden of Disease Study 2010, Lancet 380 (2012) 2224–2260.
[3] W. Tsujita, A. Yoshino, H. Ishida, T. Moriizumi, Gas sensor network for air-pollution monitoring, Sens. Actuators B: Chem. 110 (2005) 304–311.
[4] M. Lösch, M. Baumbach, A. Schütze, Ozone detection in the ppb-range with improved stability and reduced cross sensitivity, Sens. Actuators B: Chem. 130 (2008) 367–373.
[5] M. Bart, D.E. Williams, B. Ainslie, I. McKendry, J. Salmond, S.K. Grange, et al., High density ozone monitoring using gas sensitive semi-conductor sensors in the lower fraser valley, British Columbia, Environ. Sci. Technol. 48 (2014) 3970–3977.
[6] L. Deville Cavellin, S. Weichenthal, R. Tack, M.S. Ragettli, A. Smargiassi, M. Hatzopoulou, Investigating the use of portable air pollution sensors to capture the spatial variability of traffic-related air pollution, Environ. Sci. Technol. 50 (2016) 313–320.
[7] B.J. Nathan, L.M. Golston, A.S. O'Brien, K. Ross, W.A. Harrison, L. Tao, et al., Near-field characterization of methane emission variability from a compressor station using a model aircraft, Environ. Sci. Technol. 49 (2015) 7896–7903.
[8] M.J. Nieuwenhuijsen, D. Donaire-Gonzalez, I. Rivas, M. de Castro, M. Cirach, G. Hoek, et al., Variability in and agreement between modeled and personal continuously measured black carbon levels using novel smartphone and sensor technologies, Environ. Sci. Technol. 49 (2015) 2977–2982.
[9] A. Lewis, P. Edwards, Validate personal air-pollution sensors, Nature 535 (2016) 3.
[10] K.R. Smith, P.M. Edwards, M.J. Evans, J.D. Lee, M.D. Shaw, F. Squires, et al., Clustering approaches to improve the performance of low cost air pollution sensors, Faraday Discuss. 200 (2017) 621–637.
[11] A.C. Lewis, J.D. Lee, P.M. Edwards, M.D. Shaw, M.J. Evans, S.J. Moller, et al., Evaluating the performance of low cost chemical sensors for air pollution research, Faraday Discuss. 189 (2016) 85–103.
[12] M.I. Mead, O.A.M. Popoola, G.B. Stewart, P. Landshoff, M. Calleja, M. Hayes, et al., The use of electrochemical sensors for monitoring urban air quality in low-cost, high-density networks, Atmos. Environ. 70 (2013) 186–203.
[13] X. Pang, M.D. Shaw, A.C. Lewis, L.J. Carpenter, T. Batchellier, Electrochemical ozone sensors: a miniaturised alternative for ozone measurements in laboratory experiments and air-quality monitoring, Sens. Actuators B: Chem. 240 (2017) 829–837.
[14] O.A.M. Popoola, G.B. Stewart, M.I. Mead, R.L. Jones, Development of a baseline-temperature correction methodology for electrochemical sensors and its implications for long-term stability, Atmos. Environ. 147 (2016) 330–343.
[15] R. Piedrahita, Y. Xiang, N. Masson, J. Ortega, A. Collier, Y. Jiang, et al., The next generation of low-cost personal air quality sensors for quantitative exposure monitoring, Atmos. Meas. Tech. 7 (2014) 3325–3336.

[16] M. Kamionka, P. Breuil, C. Pijolat, Calibration of a multivariate gas sensing device for atmospheric pollution measurement, Sens. Actuators B: Chem. 118 (2006) 323–327.
[17] M. Mead, O. Popoola, G. Stewart, P. Landshoff, M. Calleja, M. Hayes, et al., The use of electrochemical sensors for monitoring urban air quality in low-cost, high-density networks, Atmos. Environ. 70 (2013) 186–203.
[18] T.J. Roberts, C.F. Braban, C. Oppenheimer, R.S. Martin, R.A. Freshwater, D.H. Dawson, et al., Electrochemical sensing of volcanic gases, Chem. Geol. 332–333 (2012) 74–91.
[19] J.D. Lee, S.J. Moller, K.A. Read, A.C. Lewis, L. Mendes, L.J. Carpenter, Year-round measurements of nitrogen oxides and ozone in the tropical North Atlantic marine boundary layer, J. Geophys. Res.: Atmos. 114 (2009), http://dx.doi.org/10.1029/2009JD011878.

Biographies

Xiaobing Pang is a professor in Nanjing University of Information Science and Technology. He worked previously as a research fellow in the Wolfson Atmospheric Chemistry Laboratories, Department of Chemistry, University of York, UK. He obtained his Ph. D. on environmental science from the University of Chinese Academy of Sciences and Research Centre of Eco-Environmental Sciences, CAS, in 2007. His research interests focus on the development of state-of-art techniques for atmospheric compositions including microfluidic technique, gas sensor, etc.

Marvin D. Shaw is a research scientist at the National Centre for Atmospheric Science in the Wolfson Atmospheric Chemistry Laboratories, Department of Chemistry, University of York, UK. He obtained his Ph. D. from the University of York in 2011.

Stefan Gillot was an undergraduate in the Department of Chemistry, University of York, UK.

Alastair C. Lewis is the associated director of the National Centre for Atmospheric Science, UK, and the professor of atmospheric chemistry at the University of York, UK.